Supplemental Materials

Supplemental Figure Legends

Supplemental Figure S1

Systematic analyses of the most productive DSB sites for hFACT-nucleosome complexes.

(A) Gel filtration assay of histone octamer mixed with hFACT.

Protein mixtures with stoichiometric amounts were eluted from a Superdex 200 10/300 column in 500 mM NaCl. Under these conditions, a histone octamer disintegrated into the H2A-H2B dimer and H3-H4 tetramer without hFACT. In contrast, the histone octamer mixed with hFACT was eluted as the complex of hFACT with a histone hexamer. The H2B/H4 values from the SDS-PAGE band intensity indicate that one H2A-H2B dimer is evicted from octamer by hFACT.

(B) A series of nucleosomes containing a single DSB site at different positions.

In upper panel, the DSB sites in nucleosome are marked on 145-bp 601 DNA sequence by arrowheads. In lower panel, electrophoretic assays exhibit maintenance and alteration of DSB nucleosome structures. DSBs at the direct contact site with the H2B N-tail (122/23-bp and 23/122-bp DSB) cause nucleosome deformation, suggesting that the H2B N-tail is crucial for stabilizing the nucleosome structure. Thus, these DSB nucleosomes were not used in subsequent experiments. DSBs in the right half of the 601 DNA segment (601R) decreased ratios of nucleosome formation in comparison with DSBs in the left half of 601 (601L). This agrees with the previous report, describing that 601L has a higher affinity for the histone octamer than 601R (Chua et al. 2012).

(C) Ratios of complexes of DSB nucleosomes with hFACT (blue) or hMid-AID (pink), derived from the EMSA data represented in (D) and Fig. 1D. Data are mean and s.d. for each data point, n=3. ND, not determined; band intensities of complexes are below our detection limit. hFACT and hMid-AID almost equally form complexes at three DSB sites in 601R (92/53-bp, 102/43-bp, 112/33-bp). These DSB sites in 601R destabilize nucleosome structures, as

shown in (B). Thus, hFACT appears to be more accessible to these unstable nucleosomes, which are not included in subsequent experiments.
(D) EMSAs detect complexes of hFACT or hMid-AID with DSB nucleosomes at positions in 601R of (B), and hexasome formation upon addition of hFACT or hMid-AID.
(E) The N-terminal tails of H2B pass between two gyres of the nucleosomal DNA in the human nucleosome structure (PDB code 2CV5). Arrows represent DSB sites. Histone octamer in nucleosome is shown as an electrostatic potential surface, colored between -3.0 kT/e (red) and 3.0 kT/e (blue). The electrostatic potential was calculated using APBS (Baker et al. 2001).

Supplemental Figure S2

Comparison of the hMid and hMid-AID/$(H3\text{-}H4)_2$ complex structures with other related structures.
(A) Alignment of the Mid structures from human (green, this work), *S. cerevisiae* (cyan, PDB code 4IOY), and *C. thermophilum* (pink, PDB code 4KHA; the complex with H2A-H2B (yellow and red)).
(B, C) Alignments of the H3-H4 complex structures with FACT and other chaperones ((B) DAXX, PDB code 4HGA, HJURP, PDB code 3R45, and Asf1/CIA1, PDB code 2HUE, (C) Spt2, PDB code 5BS7, and MCM2, PDB code 5BNV). hMid-AID, H3, H3', H4, H4' and the other chaperones are colored in pink, cyan, blue, yellow green, green, and gray, respectively. Red boxes show the two binding sites in the hMid-AID/$(H3\text{-}H4)_2$ complex. They are aligned with the H3'-H4' dimer (upper panel of (B)) or with H3-H4 (lower panel of (B)). Amino acid sequences of (C) represent residues on site 1 of each chaperone.
(D) Superposition between a hMid backbone structure in the isolated form (light green) and that in the complex with $(H3\text{-}H4)_2$ (pink). R.m.s.d. of 1.11 Å on 265 Cα-atoms. Dotted lines indicate disordered regions.
(E) Superposition between a $(H3\text{-}H4)_2$ backbone structure in nucleosome (yellow) and that in the complex with hMid-AID (cyan). R.m.s.d. of 1.42 Å on 284 Cα-atoms. Dotted lines indicate disordered regions. Red dotted boxes

show the two binding sites (site 1 and site 2).

Supplemental Figure S3

Electron-density maps for X-ray structures and analysis of the two binding surfaces in the hMid-AID/$(H3\text{-}H4)_2$ complex.

(A) A close-up stereo view of the final electron-density map of hMid alone contoured at 1.1 s. The final model is shown as a stick model and the water molecules as light pink spheres.

(B) A stereo view of the final electron-density map of site 2 in the hMid-AID/$(H3\text{-}H4)_2$ complex. The electron-density maps are contoured at 1.3 s, and the final coordinates are represented with colors as in Fig. 2A.

(C) Electrostatic surfaces of two binding sites in the complex. Red dotted boxes show the two binding sites. In upper panel, $(H3\text{-}H4)_2$ is represented in a ribbon model colored as in Supplemental Fig. S2B, while hMid is shown as an electrostatic potential surface. In lower panel, hMid is represented in ribbon model (pink), while $(H3\text{-}H4)_2$ is a surface model. The electrostatic surfaces are colored as in Supplemental Fig. S1E.

(D) The side chain of Leu852 of hMid-AID is flipped out to generate hydrophobic interactions with the Val101 side chain of H3 in site 2. The hMid backbone structures are superimposed between the isolated form (gray) and the complex with $(H3\text{-}H4)_2$ (pink). $(H3\text{-}H4)_2$ in the complex is colored as in (B). Gray dashed lines show hydrogen bonds.

(E) Hydrophilic interactions accompany the rearrangements of polar side chains on the H3-H4 tetramer in site 2. The $(H3\text{-}H4)_2$ backbone structures are superimposed between nucleosome (gray) and the complex with hMid-AID (colored as in (B)).

Supplemental Figure S4

Sequence alignment of selected eukaryotic Mid-AID domains of FACT (A) and N-terminal regions of H2B (B). (A) Amino acid numbers of the binding residues at Site 1 (red) and Site 2 (blue) are marked above the alignment. The residues mutated in the previous study (Hainer et al. 2012) are marked with yellow. (B) HBR is marked by a rectangle with blue dotted lines.

Supplemental Figure S5

Raw isothermal titration calorimetry (ITC) data for the interaction between hMid-AID and $(H3\text{-}H4)_2$. ITC analysis using hMid-AID as a ligand shows an endothermic interaction with $(H3\text{-}H4)_2$ (upper left panel). ITC measurements of their mutants were performed identically. The dissociation constants of mutants were calculated on the assumption that ITC-derived *N* value is one (upper right panel and lower left panel). AID exhibits the significant thermal transition upon binding to $(H3\text{-}H4)_2$ (lower right panel). However, the dissociation constant was not correctly estimated, due to lower quality data. All measurements were performed in 750 mM NaCl and 25 mM Tris-HCl, pH7.5 at 25 °C.

Supplemental Figure S6

Gel filtration assays of hMid mixed with $(H3\text{-}H4)_2$. Protein mixtures with stoichiometric amounts were eluted from a Superdex 200 10/300 column in 750 mM NaCl. Elution profiles and the corresponding SDS-PAGE exhibit that hMid alone cannot form the complex with $(H3\text{-}H4)_2$.

Supplemental Figure S7

Representation of the docking model of nucleosome with hMid, as shown in Fig. 4A. Nucleosomes (PDB code 2CV5) are represented in ribbon models of H2B (pink), H2A (yellow), H3 (light blue), H4 (green), and DNA (gray). hMid is shown as an electrostatic potential surface, colored as in Supplemental Fig. S1E Red boxes show the locations of steric hindrance with the nucleosomal DNA.

(A) Orthogonal views of the docking model. In the back view, a black arrow indicates that a broad basic surface of hMid contacts the nucleosomal DNA around the central region. In some views, two copies of H2A-H2B and DNA bases are removed for clarity.

(B) Docking model viewed along dyad axis. Electrostatic repulsions between the hMid acidic surface and the nucleosomal DNA are highlighted.

Supplemental Figure S8

ITC measurements (A) and gel filtration assays (B) clarify the functional role of AID.

(A) ITC measurements of interactions between various FACT and H2A-H2B constructs. ITC data for the interaction between hMid-AID and H2A-H2B shows two transitions, one of which is endothermic and the other is exothermic. In agreement with this finding, a similar construct, Spt16MC, which is composed of Mid and AID, also exhibits two thermal transitions upon binding to H2A-H2B under the same conditions, as described in the previous study (Hondele et al. 2013). Importantly, AID alone, without Mid, exhibits two thermal transitions upon binding to H2A-H2B, whereas deletion mutants of AID and the H2B N-tail show no significant changes. This suggests that the H2B N-tail and AID are important for the interaction between FACT and H2A-H2B. It was impossible to estimate the dissociation constants of their interactions, possibly due to the serious aggregation of these proteins during ITC measurements. All measurements were performed in 200 mM NaCl, and 25 mM Tris-HCl, pH7.5 at 25 °C.

(B) Elution profiles and the corresponding SDS-PAGE in gel filtration assay of histone octamer mixed with AID. Protein mixtures with stoichiometric amounts were eluted from a Superdex 200 10/300 column in 500 mM NaCl. Under this condition, a histone octamer disintegrated into the H2A-H2B dimer and H3-H4 tetramer. In contrast, the mixture of AID and the histone octamer in the same buffer was eluted at the stoichiometry of the histone octamer. SDS-PAGE bands of AID are not detectable, due to the enriched negative charges of AID.

Supplemental Figure S9

Docked model of hMid-AID/$(H3\text{-}H4)_2$/MCM2 complex at 1:1:1 stoichiometry. The model (middle panel) was constructed by making the best superposition of the $(H3\text{-}H4)_2$ structure between hMid-AID/$(H3\text{-}H4)_2$ (left panel) and MCM2/$(H3\text{-}H4)_2$ (PDB code 5BNV, right panel). hMid-AID and $(H3\text{-}H4)_2$ are represented with colors as in Fig. 2A. $(H3\text{-}H4)_2$ in the middle panel is shown as a molecular surface. One MCM2 molecule (orange) could bind to

hMid-AID/$(H3\text{-}H4)_2$ with no steric hindrance. The previous study indicated that the complex of one MCM2 molecule with $(H3\text{-}H4)_2$ could sufficiently exhibit the histone chaperoning function (Huang et al. 2015).

Tsunaka_GENESDEV/2015/274183 _Supplemental Fig.S1

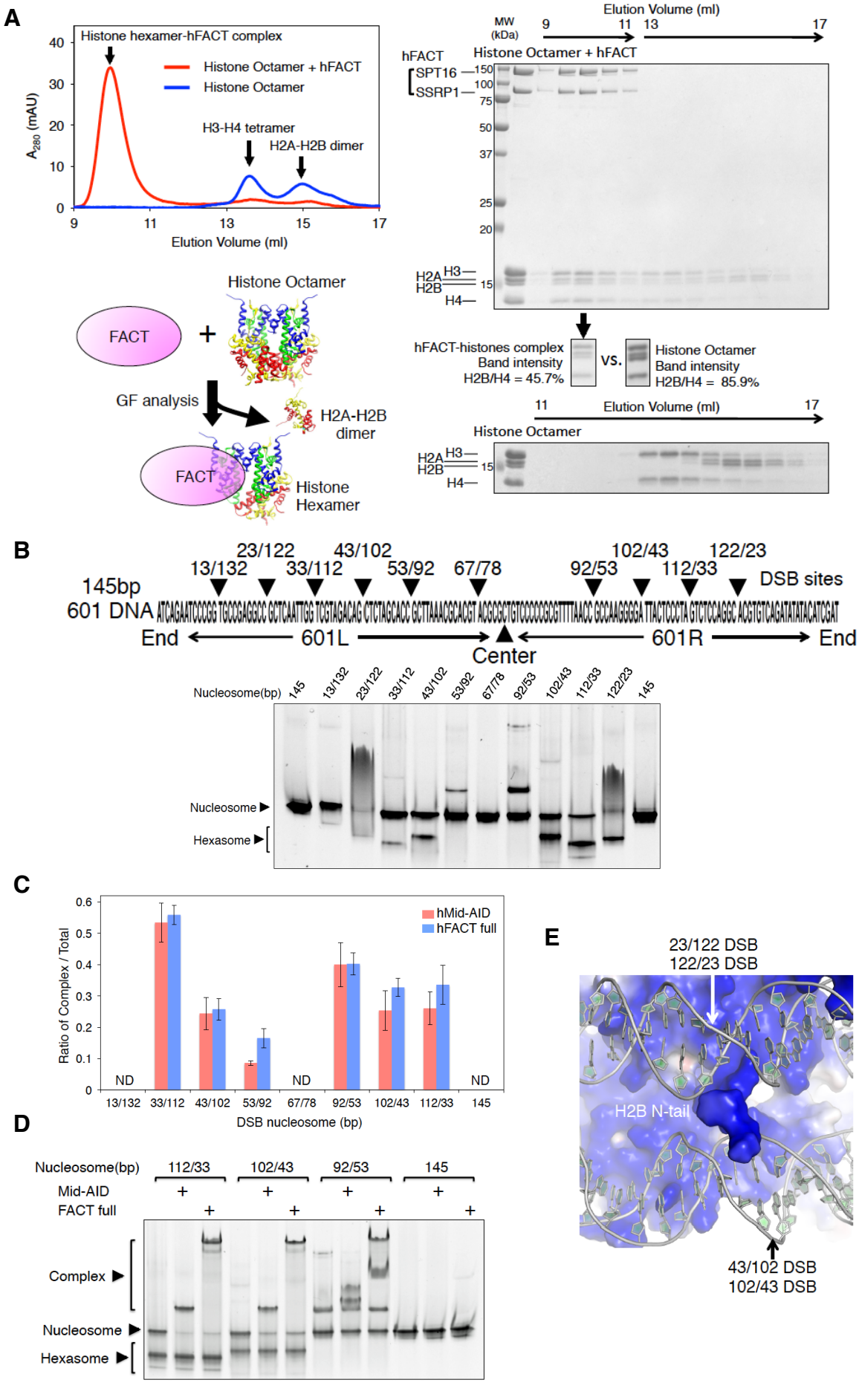

Tsunaka_GENESDEV/2015/274183 _Supplemental Fig.S2

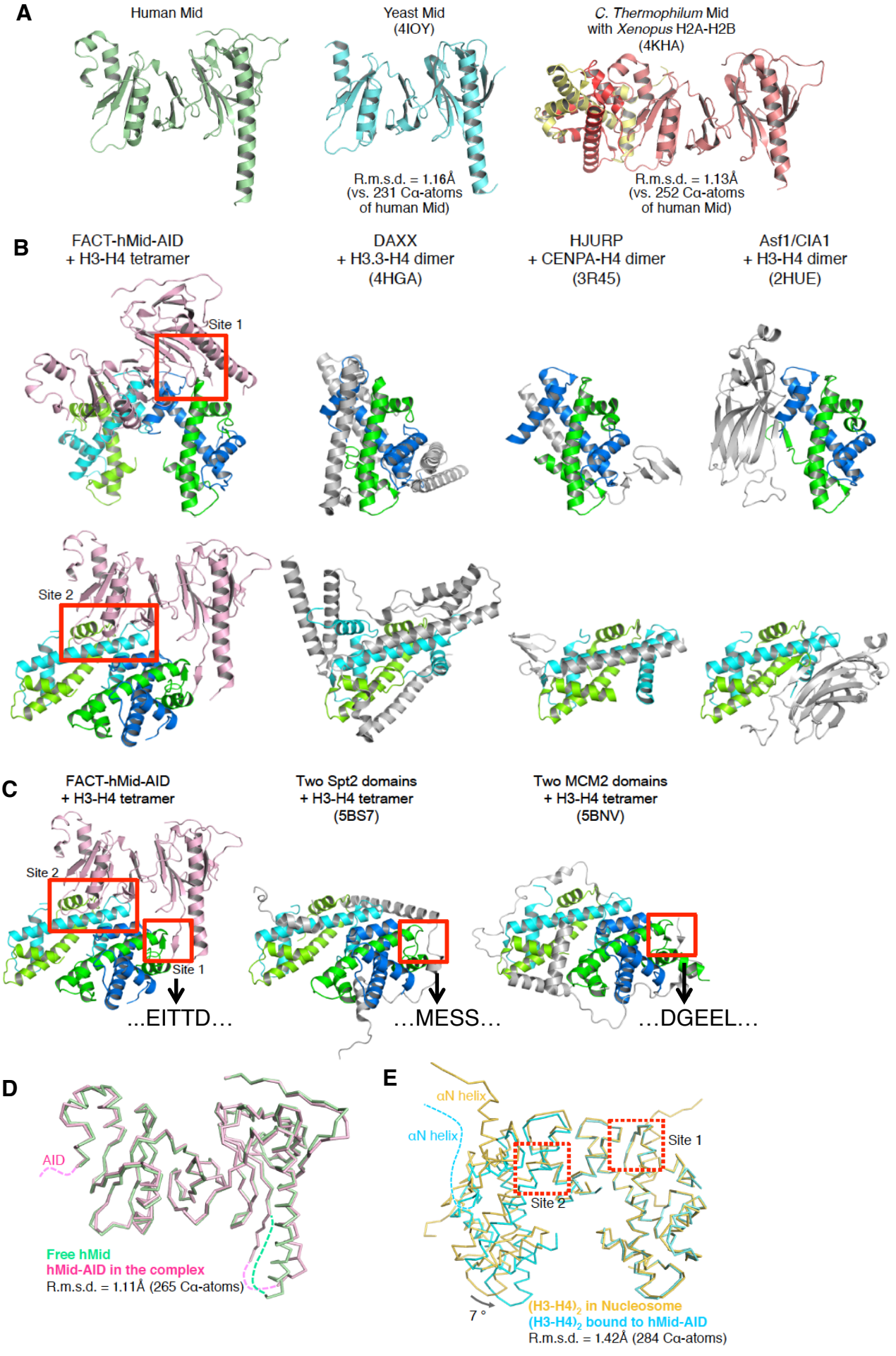

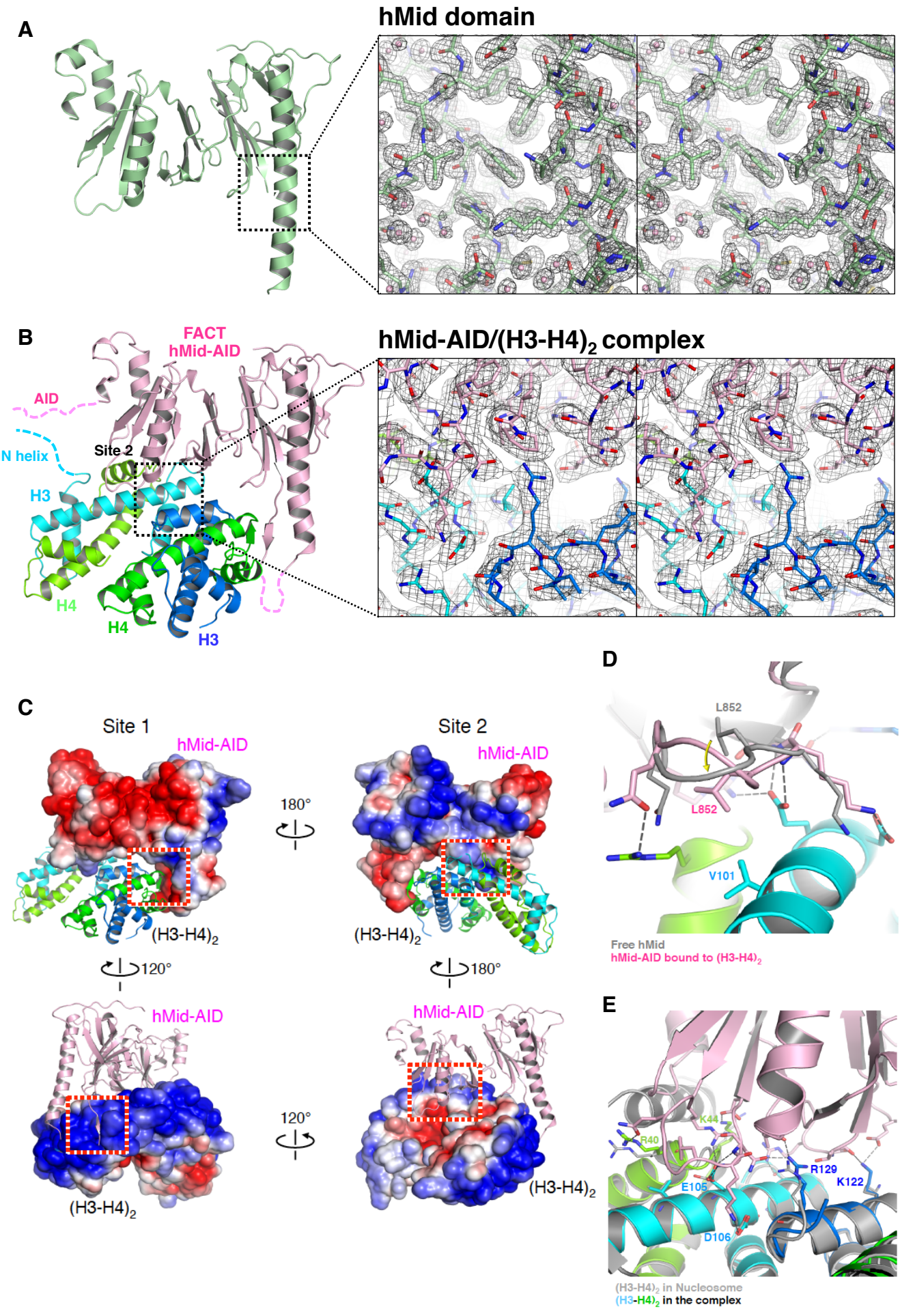
A
hMid domain
B
FACT
hMid-AID
AID
αN helix
Site 2
H3
H4
H4
H3
hMid-AID/(H3-H4)2 complex
C
Site 1
hMid-AID
(H3-H4)2
180°
Site 2
hMid-AID
(H3-H4)2
120°
180°
hMid-AID
hMid-AID
120°
(H3-H4)2
(H3-H4)2
D
L852
L852
V101
Free hMid
hMid-AID bound to (H3-H4)2
E
K44
R40
R129
K122
E105
D106
(H3-H4)2 in Nucleosome
(H3-H4)2 in the complex

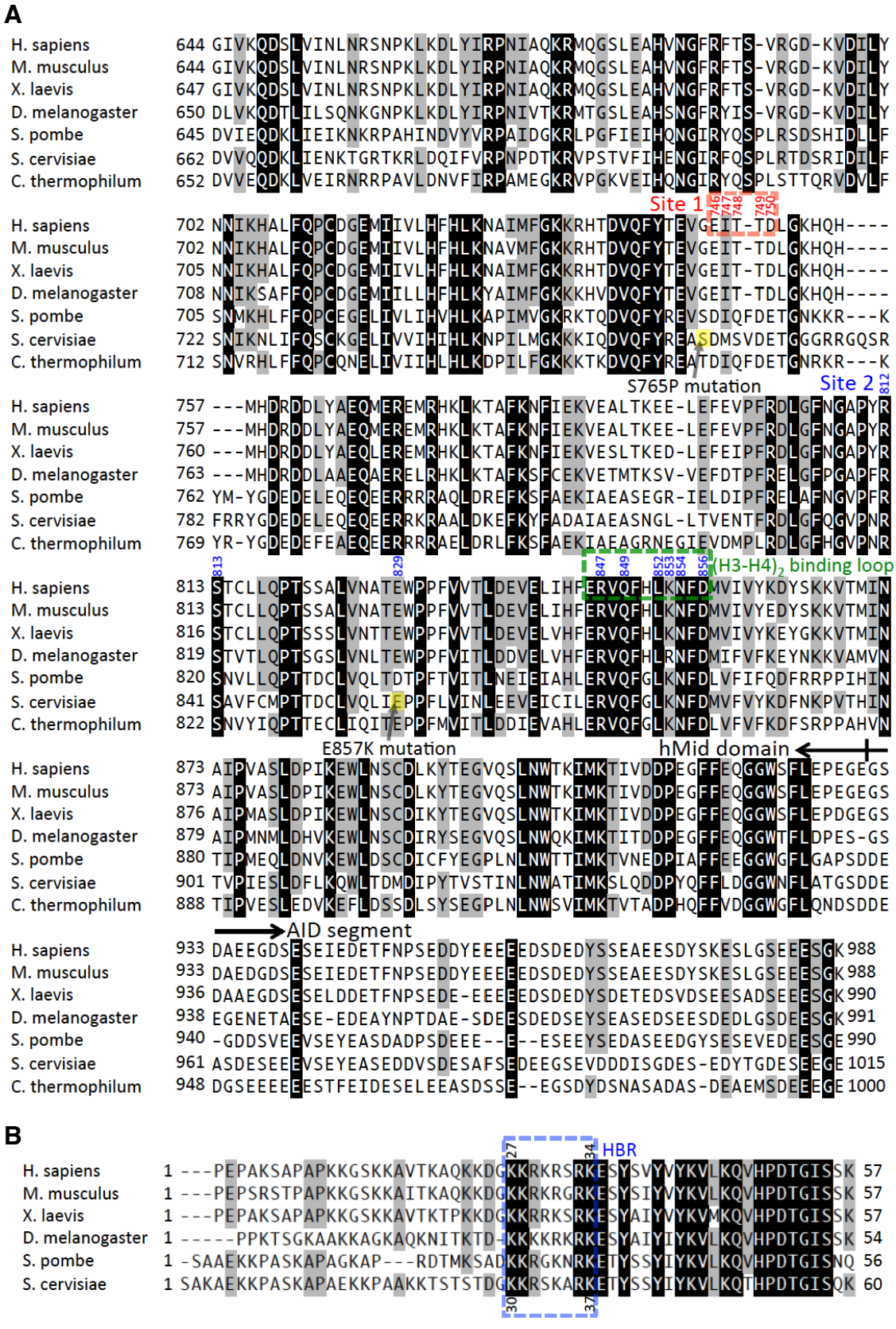
A
H. sapiens 644 GIVKQDSLVINLNRSNPKLKDLYIRPNIAQKRMQGSLEAHVNGFRFTS-VRGD-KVDILY
M. musculus 644 GIVKQDSLVINLNRSNPKLKDLYIRPNIAQKRMQGSLEAHVNGFRFTS-VRGD-KVDILY
X. laevis 647 GIVKQDSLVINLNRSNPKLKDLYIRPNIAQKRMQGSLEAHVNGFRFTS-VRGD-KVDILY
D. melanogaster 650 DLVKQDTLILSQNKGNPKLKDLYIRPNIVTKRMTGSLEAHSNGFRYIS-VRGD-KVDILY
S. pombe 645 DVIEQDKLIEIKNKRPAHINDVYVRPAIDGKRLPGFIEIHQNGIRYQSPLRSDSHIDLLF
S. cervisiae 662 DVVQQDKLIENKTGRTKRLDQIFVRPNPDTKRVPSTVFIHENGIRFQSPLRTDSRIDILF
C. thermophilum 652 DVVEQDKLVEIRNRRPAVLDNVFIRPAMEGKRVPGKVEIHQNGIRYQSPLSTTQRVDVLF
Site 1
H. sapiens 702 NNIKHALFQPCDGEMIIVLHFHLKNAIMFGKKRHTDVQFYTEVGEIT-TDLGKHQH----
M. musculus 702 NNIKHALFQPCDGEMIIVLHFHLKNAVMFGKKRHTDVQFYTEVGEIT-TDLGKHQH----
X. laevis 705 NNIKHALFQPCDGEMIIVLHFHLKNAIMFGKKRHTDVQFYTEVGEIT-TDLGKHQH----
D. melanogaster 708 NNIKSAFFQPCDGEMIILLHFHLKYAIMFGKKKHVDVQFYTEVGEIT-TDLGKHQH----
S. pombe 705 SNMKHLFFQPCEGELIVLIHVHLKAPIMVGKRKTQDVQFYREVSDIQFDETGNKKR---K
S. cervisiae 722 SNIKNLIFQSCKGELIVVIHIHLKNPILMGKKKIQDVQFYREASDMSVDETGGGRRGQSR
C. thermophilum 712 SNVRHLFFQPCQNELIVIIHLHLKDPILFGKKKTKDVQFYREATDIQFDETGNRKR---K
S765P mutation
Site 2
H. sapiens 757 ---MHDRDDLYAEQMEREMRHKLKTAFKNFIEKVEALTKEE-LEFEVPFRDLGFNGAPYR
M. musculus 757 ---MHDRDDLYAEQMEREMRHKLKTAFKNFIEKVEALTKEE-LEFEVPFRDLGFNGAPYR
X. laevis 760 ---MHDRDDLYAEQLEREMRHKLKTAFKNFIEKVESLTKED-LEFEIPFRDLGFNGAPYR
D. melanogaster 763 ---MHDRDDLAAEQAERELRHKLKTAFKSFCEKVETMTKSV-VEFDTPFRELGFPGAPFR
S. pombe 762 YM-YGDEDELEQEQEERRRAQLDREFKSFAEKIAEASEGR-IELDIPFRELAFNGVPFR
S. cervisiae 782 FRRYGDEDELEQEQEERKRAALDKEFKYFADAIAEASNGL-LTVENTFRDLGFQGVPNR
C. thermophilum 769 YR-YGDEDEFEAEQEERRRRAELDRLFKSFAEKIAEAGRNEGIEVDMPLRDLGFHGVPNR
(H3-H4)2 binding loop
H. sapiens 813 STCLLQPTSSALVNATEWPPFVVTLDEVELIHFERVQFHLKNFDMVIVYKDYSKKVTMIN
M. musculus 813 STCLLQPTSSALVNATEWPPFVVTLDEVELIHFERVQFHLKNFDMVIVYEDYSKKVTMIN
X. laevis 816 STCLLQPTSSSLVNTTEWPPFVVTLDEVELVHFERVQFHLKNFDMVIVYKEYGKKVTMIN
D. melanogaster 819 STVTLQPTSGSLVNLTEWPPFVITLDDVELVHFERVQFHLRNFDMIFVFKEYNKKVAMVN
S. pombe 820 SNVLLQPTTDCLVQLTDTPFTVITLNEIEIAHLERVQFGLKNFDLVFIFQDFRRPPIHIN
S. cervisiae 841 SAVFCMPTTDCLVQLIEPPFLVINLEEVEICILERVQFGLKNFDMVFVYKDFNKPVTHIN
C. thermophilum 822 SNVYIQPTTECLIQITEPPFMVITLDDIEVAHLERVQFGLKNFDLVFVFKDFSRPPAHVN
E857K mutation
hMid domain
H. sapiens 873 AIPVASLDPIKEWLNSCDLKYTEGVQSLNWTKIMKTIVDDPEGFFEQGGWSFLEPEGEGS
M. musculus 873 AIPVASLDPIKEWLNSCDLKYTEGVQSLNWTKIMKTIVDDPEGFFEQGGWSFLEPEGEGS
X. laevis 876 AIPMASLDPIKEWLNSCDIKYTEGVQSLNWTKIMKTIVDDPEGFFEQGGWSFLEPDGEGS
D. melanogaster 879 AIPMNMLDHVKEWLNSCDIRYSEGVQSLNWQKIMKTITDDPEGFFEQGGWTFLDPES-GS
S. pombe 880 TIPMEQLDNVKEWLDSCDICFYEGPLNLNWTTIMKTVNEDPIAFFEEGGWGFLGAPSDDE
S. cervisiae 901 TVPIESLDFLKQWLTDMDIPYTVSTINLNWATIMKSLQDDPYQFFLDGGWNFLATGSDDE
C. thermophilum 888 TIPVESLEDVKEFLDSSDLSYSEGPLNLNWSVIMKTVTADPHQFFVDGGWGFLQNDSDDE
AID segment
H. sapiens 933 DAEEGDSESEIEDETFNPSEDDYEEEEEDSDEDYSSEAEESDYSKESLGSEEESGK 988
M. musculus 933 DAEDGDSESEIEDETFNPSEDDYEEEEEDSDEDYSSEAEESDYSKESLGSEEESGK 988
X. laevis 936 DAAEGDSESELDDETFNPSEDE-EEEEEDSDEDYSDETEDSVDSEESADSEEESGK 990
D. melanogaster 938 EGENETAESE-EDEAYNPTDAE-SDEESDEDSEYSEASEDSEESDEDLGSDEESGK 991
S. pombe 940 -GDDSVEEVSEYEASDADPSDEEE--E--ESEEYSEDASEEDGYSESEVEDEESGE 990
S. cervisiae 961 ASDESEEEVSEYEASEDDVSDESAFSEDEEGSEVDDDISGDES-EDYTGDESEEGE 1015
C. thermophilum 948 DGSEEEEEESTFEIDESELEEASDSSE--EGSDYDSNASADAS-DEAEMSDEEEGE 1000
B
HBR
H. sapiens 1 ---PEPAKSAPAPKKGSKKAVTKAQKKDGKKRKRSRKESYSVYVYKVLKQVHPDTGISSK 57
M. musculus 1 ---PEPSRSTPAPKKGSKKAITKAQKKDGKKRKRGRKESYSIYVYKVLKQVHPDTGISSK 57
X. laevis 1 ---PEPAKSAPAPKKGSKKAVTKTPKKDGKKRRKSRKESYAIYVYKVMKQVHPDTGISSK 57
D. melanogaster 1 -----PPKTSGKAAKKAGKAQKNITKTD-KKKKRKRKESYAIYIYKVLKQVHPDTGISSK 54
S. pombe 1 -SAAEKKPASKAPAGKAP---RDTMKSADKKRGKNRKETYSSYIYKVLKQVHPDTGISNQ 56
S. cervisiae 1 SAKAEKKPASKAPAEKKPAAKKTSTSTDGKKRSKARKETYSSYIYKVLKQTHPDTGISQK 60

Tsunaka_GENESDEV/2015/274183 _Supplemental Fig.S5

hMid-AID + H3-H4

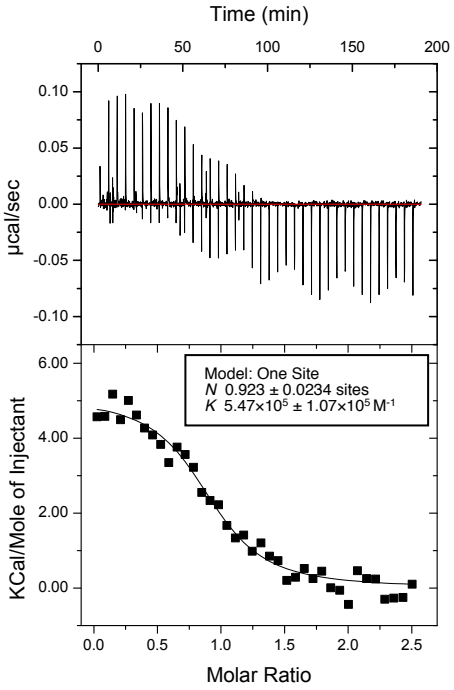

hMidm1m2-AID + H3-H4

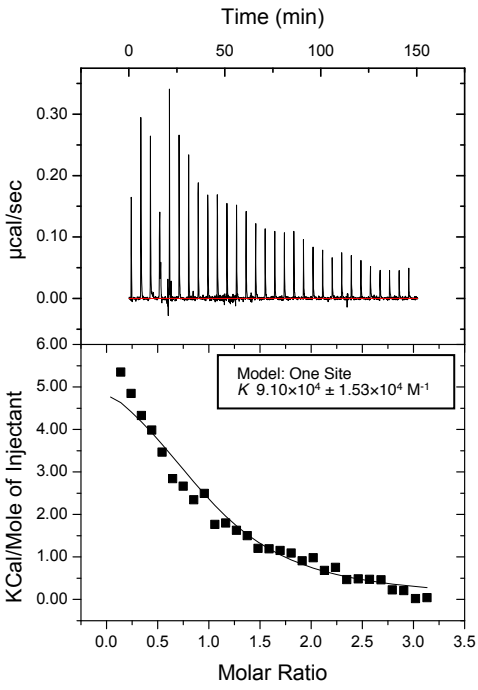

hMid-AID + H3m2-H4

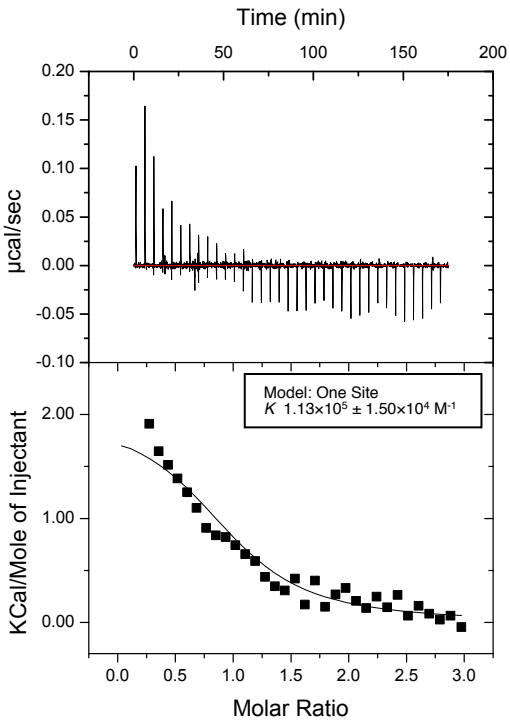

AID + H3-H4

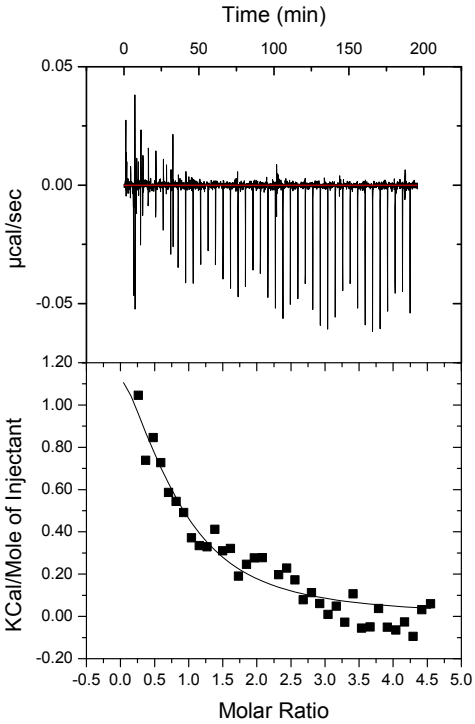

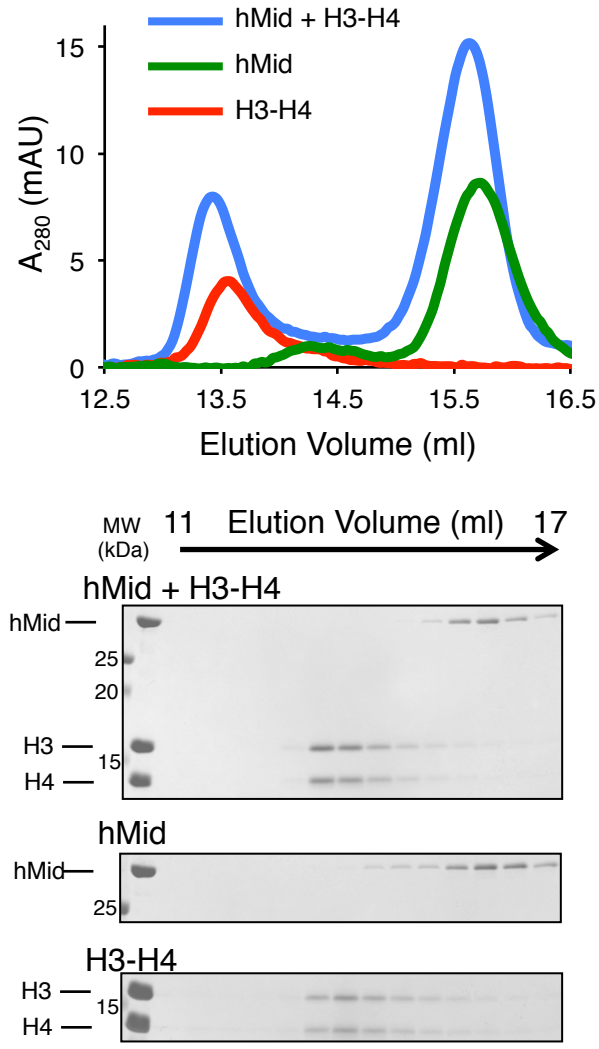
hMid + H3-H4
hMid
H3-H4
15
10
5
0
A_{280} (mAU)
12.5
13.5
14.5
15.5
16.5
Elution Volume (ml)
MW
(kDa)
11
Elution Volume (ml)
17
hMid + H3-H4
hMid
25
20
H3
H4
15
hMid
hMid
25
H3-H4
H3
H4
15

Tsunaka_GENESDEV/2015/274183 _Supplemental Fig.S7

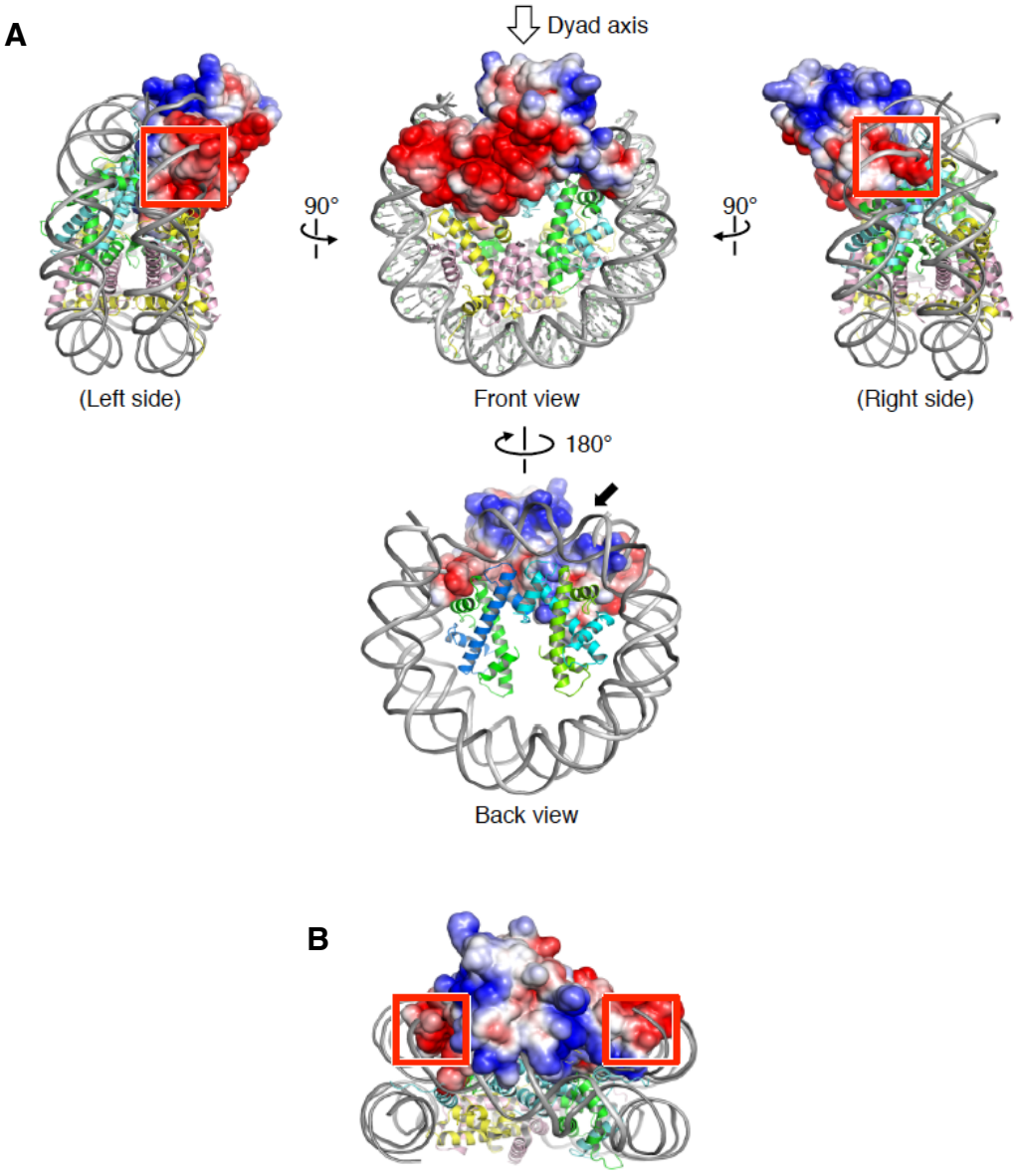

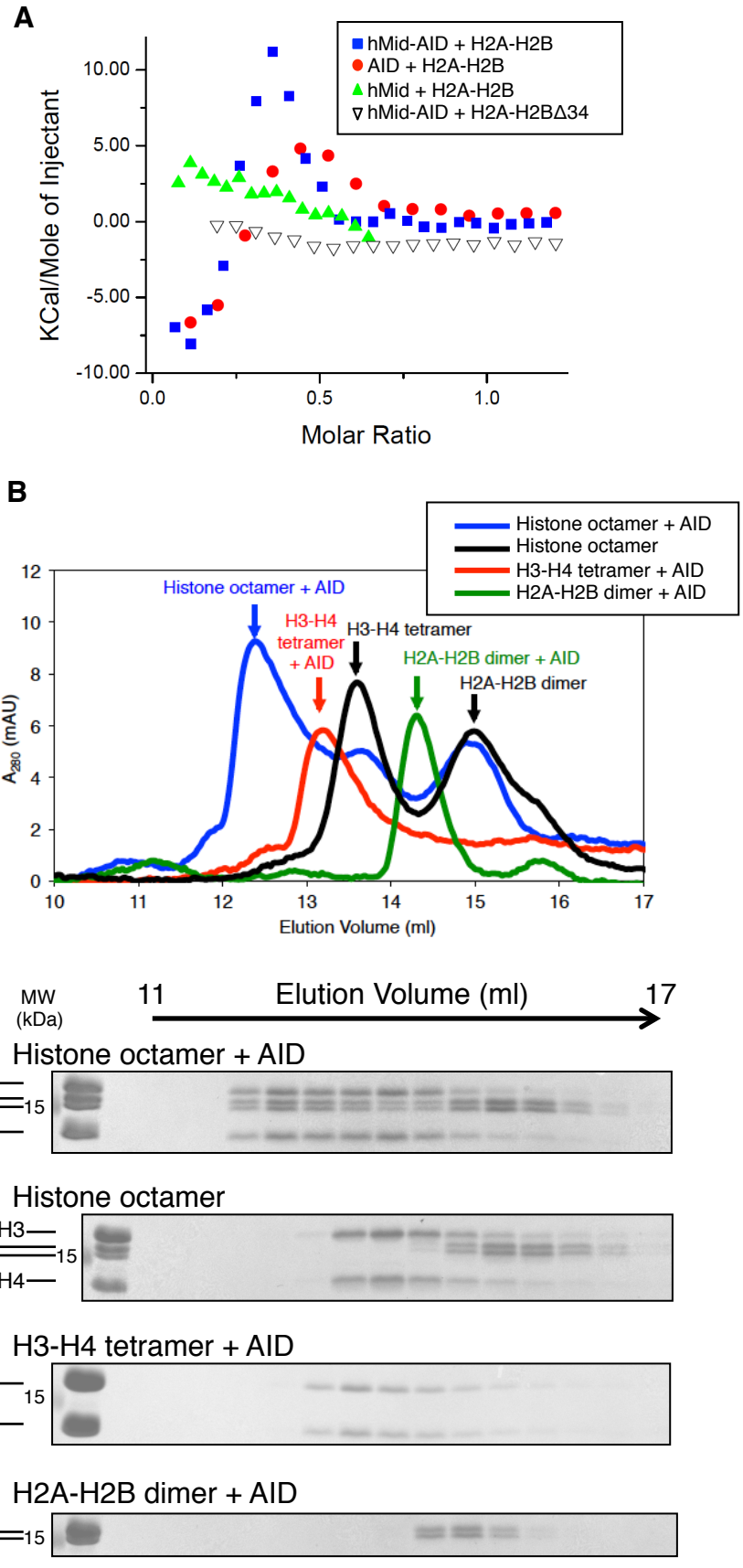
A
hMid-AID + H2A-H2B
AID + H2A-H2B
hMid + H2A-H2B
hMid-AID + H2A-H2BΔ34
KCal/Mole of Injectant
10.00
5.00
0.00
-5.00
-10.00
0.0
0.5
1.0
Molar Ratio
B
Histone octamer + AID
Histone octamer
H3-H4 tetramer + AID
H2A-H2B dimer + AID
Histone octamer + AID
H3-H4 tetramer + AID
H3-H4 tetramer
H2A-H2B dimer + AID
H2A-H2B dimer
A280 (mAU)
Elution Volume (ml)
MW (kDa)
11
Elution Volume (ml)
17
Histone octamer + AID
H2A
H2B
H3
H4
15
Histone octamer
H3-H4 tetramer + AID
H2A-H2B dimer + AID

Tsunaka_GENESDEV/2015/274183 _Supplemental Fig.S9